

# Ant Colony Optimization Tuned Fuzzy Control for PV Battery and Super Capacitor Powered Electric Vehicle

<sup>1</sup>Ankita Maurya, <sup>2</sup>Jaya Shukla

Submitted: 07/05/2024 Revised: 20/06/2024 Accepted: 28/06/2024

**Abstract:** This study presents a control plan for a photovoltaic (PV) battery and supercapacitor-powered electric vehicle (EV) using ant colony optimization (ACO) tuned fuzzy control. The proposed approach utilizes the ACO algorithm to optimize the parameters of the fuzzy controller, which is designed to manage the power flow between the electric motor, supercapacitor, and PV battery. The fuzzy control system takes into account the vehicle's speed, battery and supercapacitor voltages, and the power demand from the motor to decide the optimal power delivery among the energy storage devices. The results obtained by Simulation show that the proposed ACO tuned fuzzy control approach effectively advances the vehicle's performance and achieves better energy management. The optimization of the proposed Ant colony optimization based Fuzzy control was examined and its performance investigated through MATLAB/Simulink.

**Keywords:** Ant colony Optimization, Fuzzy, PV, Battery, EV.

## Introduction

Due to its reputation for sustainability and cleanliness, photovoltaic (PV) expertise has emerged as a preferred kind of renewable energy technology [1]. The output voltage, power, and frequency may vary excessively due to the PV energy's irradiance volatility. Active generators, on the other hand, may offer a reserve of energy with less fluctuating power thanks to the use of storage devices in their design [2-4].

Modern batteries provide better energy storage density and good discharge efficiency, but they have a comparatively less energy density. Low internal resistance is a property of supercapacitors (SCs). Therefore, a SC and Battery combination may reduce the rate volume impact of high release of discharge current [5]. Therefore, SCs are presently employed in Nonconventional energy [6, 7] and power systems [8] as temporary power shields or secondary energy storage devices. The activity of the batteries dynamically and their extended life, this grouping is in fact an intriguing way to enhance system performance [9]. The development of this battery and SC combo proved successful.

The solution to the power management issue and the power spreading between batteries and SCs is a fuzzy logic-based algorithm. However, unlike traditional control, the fuzzy logic monitor does not need sophisticated scientific representations. Energy management systems (EMS) are already controlled by FLS in several applications, such as EMS for poly generation microgrids. [10]

Ant Colony Optimisation (ACO) is a discrete optimisation procedure that draws its inspiration from the scavenging habits of ant colonies [11]. The values set for the ACO algorithm's parameters, which affect its convergence, have a significant impact on how the algorithm behaves. Typically, these are maintained constant while the algorithm is running. The algorithm's performance may be enhanced by altering the parameters while it is running, at a certain moment, or in response to the progress of the search [12–14]. focus on the areas where suitable solutions may be discovered. In the use of fuzzy techniques and ANFIS, neural network has arisen as one of the most energetic and productive fields of study. When procedures are too complicated for study by normal quantitative approaches or when the causes of evidence supplied are perceived in a qualitatively wrong or unclear manner, fuzzy logic controllers' methodology might be helpful [15].

It is a difficult issue that takes a lot of time to solve to choose the right settings for the fuzzy logic controller. The selection of the ACO for previously stated parameters because of their capacity to handle complicated NP-hard situations.

## Proposed System

The System Comprises of Solar PV Array, Battery & a Super Capacitor linked to the DC bus, Here the PV system is connected through a Boost converter to the bus, Battery and Supercapacitor is associated to DC bus through a Bidirectional DC to DC Converter. The representation of the system is shown in Figure 1.

<sup>1,2</sup>Dept of Electrical Engineering, Vbs Purvanchal University Jaunpur.

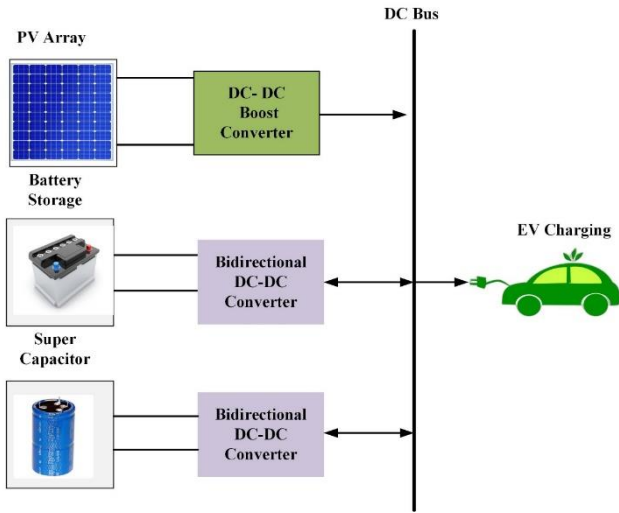


**Fig 1** Block Diagram of the PV, Super Capacitor & battery Connected to DC bus

### PV Model

Fig.2 depicts a straightforward equivalent circuit model for a solar cell. The components of the model include a source current  $I_{ph}$  (which represents photo current of the cell), a series resistance  $R_s$  (which represents each cell's internal resistance), and a diode. The following equation defines the photovoltaic cell's net output current. The difference between the  $I_{ph}$  and the  $I_D$  is shown in the equation(1).

$$I_s = I_{ph} - I_D = I_{ph} - I_o \left( e^{\left( \frac{q(V_s + I_s R_s)}{mKT} \right)} - 1 \right) \quad (1)$$

where  $q$  is the electron charge,  $T$  is the absolute temperature of the cell,  $m$  is the ideality factor of the diode,  $k$  is Boltsmann's constant,  $V_s$  is the applied voltage across the cell, and  $I_o$  is the saturation current. A PV module is created by joining the cells in parallel and series.

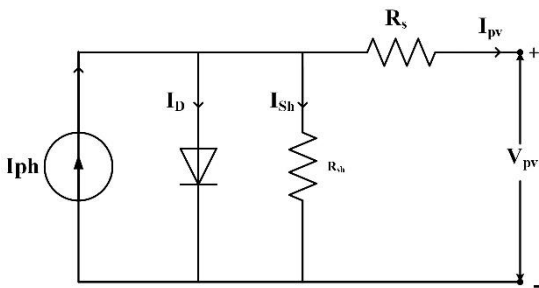


**Fig 2.** Equivalent Circuit of PV Cell

### Battery Model

The analysis of batteries in PV systems is crucial for evaluating the consequence of various charging rates, state of charge (SOC), and state of health (SOH) on their performance as the primary storage medium. To determine the optimal battery size for a specific application, various testing scenarios can be employed. Simulations offer a cost-

effective means of comparing different storage options deprived of the requirement for expensive test setups.

Fig.3 depicts a straightforward equivalent circuit battery concept. The Battery state of charge (SOC) & depth of charge of the battery (DOC) are both considered by the battery model. The battery DOC calculated the percentage of the charge of battery to working volume. The battery's operating ability decreases with increased current discharge. The model has two RC parallel branches, internal resistance  $R_0$ , and an battery voltage during open circuit of  $E_{oc}$ . Here are the model equations: (2)–(6).

$$E_{oc} = E_o - (1 - SOC)K_e \quad (2)$$

$$R_1 = R_{10}e^{-(1 - SOC)K_e} \quad (3)$$

$$R_2 = \frac{R_{20}}{DOC} \quad (4)$$

$$SOC = 1 - \frac{1}{C_n} \int i_{batt} d\tau \quad (5)$$

$$DOC = 1 - \frac{1}{C(i_{avg})} \int i_{batt} d\tau \quad (6)$$

where: SOC battery state of charge

DOC battery deep of charge

$C_n$  is the capacity of battery

$C(i_{avg})$  is the current-dependent battery capacity

$E_o$  is Maximum charged OCC Voltage

$K_e$  is a constant

$R_{10}$  is the Constant of RC branch constant in  $\Omega$

$\tau_1$  is the Time constant of RC branch in sec

$K_1$  is a constant

$R_{20}$  is the Constant of RC branch in  $\Omega$

$\tau_2$  is the Time constant of RC branch in sec

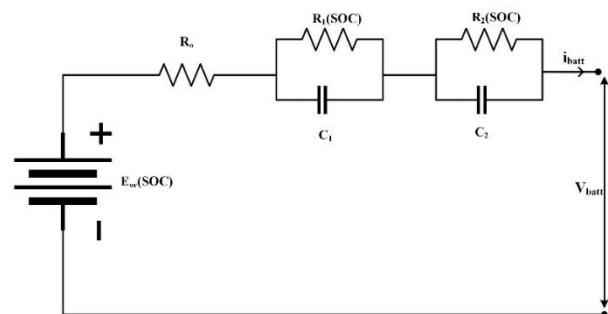


**Fig 3.**Equivalent Circuit Model of Battery

### Supercapacitor Model

The supercapacitor's traditional comparable circuit concept is seen in Fig.4. The equivalent series and parallel resistance (EPR and ESR) & capacitance, are the three parts that make up the model. During charging and

discharging, the ESR, a cost term that represents interior temperature increase in the capacitor, is crucial. The supercapacitor's long-term energy storage capability will be impacted by the current leakage effect, which is modelled by the EPR, where C is capacitance. The ESR, EPR, and supercapacitor voltage at terminal are described in equations (7) through (9).

$$ESR = \frac{\Delta v}{\Delta i} \quad (7)$$

$$EPR = \frac{-(t_2 - t_1)}{\ln\left(\frac{V_2}{V_1}\right)C} \quad (8)$$

$$v_c = ESR \cdot i_c + \frac{1}{C} \int \left( i_c - \frac{e_c}{EPR} \right) d\tau + V_{c\_init} \quad (9)$$

where: V1 is the Starting self-discharge voltage at t1

V2 is the ending self-discharge voltage at t2

C is the rated value of the capacitance

$\Delta V$  change in voltage

$\Delta I$  change in current

$V_{c\_init}$  voltage at the capacitor

$i_c$  is the current at the capacitor

By analyzing the charging and discharging measurements through curve fitting, one can dependent on voltage.

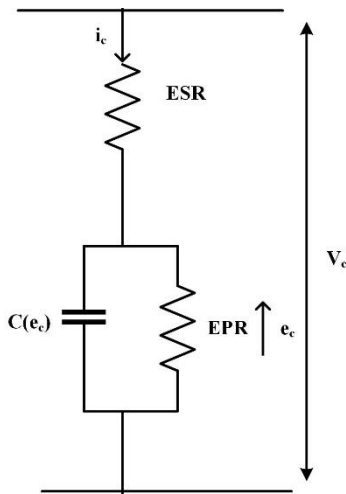


Fig 4 Equivalent Circuit Model of Super Capacitor

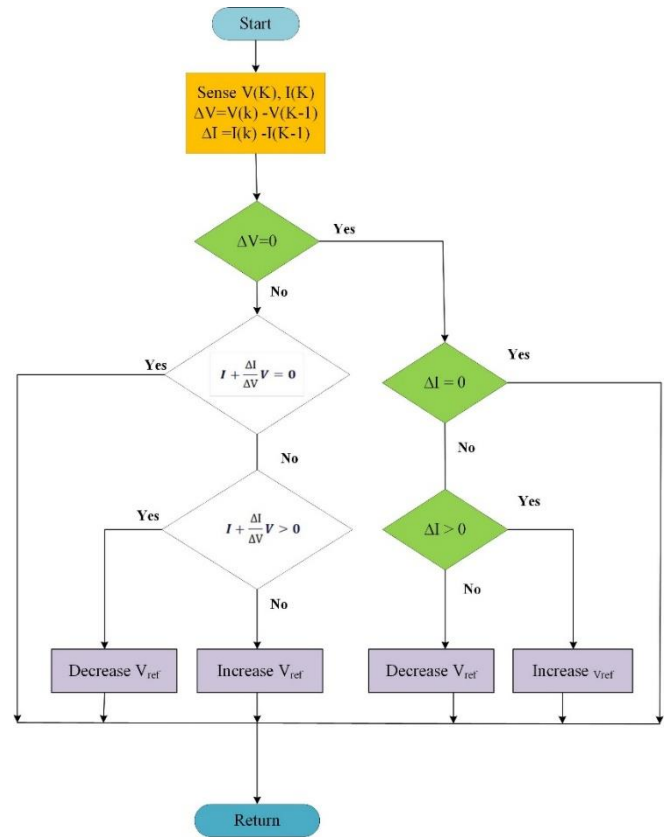


Fig 5. Flow Chart of Incremental Conductance MPPT

### Incremental Conductance MPPT

The use of the IC method addresses the limitations of the perturb and observe technique in tracking the maximum power point (MPP) under dynamic atmospheric conditions. Once the IC detects that the MPP has been attained, it can discontinue perturbing the operating point. By utilizing the relationship between  $dI/dV$  and  $-I/V$ , it is possible to ascertain the appropriate direction to perturb the operating point of the maximum power point tracker (MPPT) if this criterion is not met. This connection was established based on the observation that  $dP/dV$  is negative when the MPPT is located to the right side of the MPP and positive when it is to the left side of the MPP. Compared to the perturb and observe (P&O) technique, which exhibits oscillatory behavior around the MPP, this algorithm possesses the advantage of being able to detect when the MPPT has attained the MPP. Furthermore, incremental conductance is superior to P&O in accurately following rapidly fluctuating irradiance conditions.

As a function of voltage, the current in the array may be visualised as follows:  $P=I(V)V$ . Therefore,

$$\frac{dP}{dV} = v \frac{dI}{dV} + I(v) \quad (10)$$

Setting this equal to zero gives

$$\frac{dI}{dV} = -I(v)v \quad (11)$$

The point of maximum power (MPP) can be determined by finding the point where the incremental conductance equals the negative value of the instantaneous conductance. Based on the characteristics of the power-voltage curve, if the voltage is below the MPP, this relationship holds true.,

$$\frac{dP}{dV} > 0 \quad (12)$$

So

$$\frac{dP}{dV} > \frac{-I}{v} \quad (13)$$

when MPP is less than the voltage,

$$\frac{dP}{dV} < 0 \quad (14)$$

or

$$\frac{dI}{dV} > \frac{-I}{v} \quad (15)$$

To determine its position on the power-voltage curve, a tracker can evaluate the correlation between the voltage or current values and their respective changes.

### Ant Colony Optimization

Ant Colony Improvement The travelling salesman problem (TSP), which seeks to determine the easiest path between many cities, was the primary purpose of the original ACO algorithm, known as Ant System (AS). Each ant builds a full solution iteratively by continuously adding pieces. The next piece to be added is selected based on a probability that relies on two variables. the heuristic factor,

which assesses the curiosity of choosing a component with regard to an unbiased function, and the pheromone factor, which represents the colony's historical experience. Each parameter weighs the two elements differently.

$$P_{ij}^k = \frac{[\tau_{ij}]^\alpha [\eta_{ij}]^\beta}{\sum_{l \in N_i^k} [\tau_{il}]^\alpha [\eta_{il}]^\beta}, \text{ if } j \in N_i^k \quad (16)$$

The connection between nodes i and j is represented by Formula (16), which involves  $\eta_{ij}$  as a heuristic parameter indicating the attractiveness of choosing a component based on an objective function. Moreover,  $N_i$  specifies the area adjacent to node i. Following the completion of all ant tours, the pheromone paths are updated by reducing the pheromone level on all edges by a constant factor. This approach controls the buildup of pheromone trails and ensures that the algorithm avoids repeating erroneous decisions.

$$\tau_{ij} \leftarrow (1-\rho)\tau_{ij}, \forall (i, j) \in L \quad (17)$$

Additionally, by leaving pheromone behind on the arcs that ants have travelled (3). The quantity of pheromone that the arcs will get will increase with how well the tour goes. In (2), the variable  $\rho$  denotes the pheromone evaporation rate, which ranges from 0 to 1.

$$\tau_{ij} \leftarrow \tau_{ij} + \sum_{k=1}^n \Delta\tau_{ij}^k, \forall (i, j) \in L$$

$$\Delta\tau_{ij}^k = \begin{cases} \frac{1}{c^k}, & \text{if arc}(i, j) \text{ belong to } T^k; \\ 0, & \text{otherwise;} \end{cases} \quad (18)$$

$c$  in (3) stands for the arc's cost on a graph. The exclusive approach for Ant System (EAS), which is a first advancement over the original AS, is as follows. The goal is to provide the arcs fitting to the best tour discovered since the procedure's inception substantial extra reinforcement. .

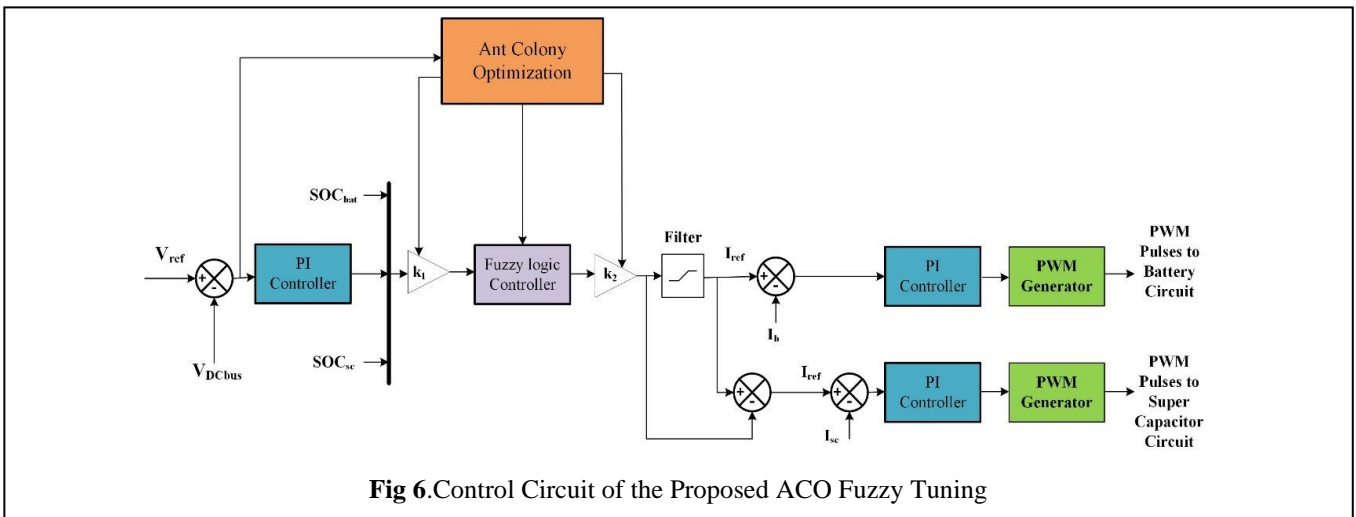


Fig 6. Control Circuit of the Proposed ACO Fuzzy Tuning

$$\tau_{ij} \leftarrow \tau_{ij} + \sum_{k=1}^n \Delta\tau_{ij}^k + e\Delta\tau_{ij}^{bs}, \forall (i,j) \in L$$

$$\Delta\tau_{ij}^{bs} = \begin{cases} \frac{1}{c^{bs}}, & \text{if } arc(i,j) \text{ belong to } T^{bs}; \\ 0, & \text{otherwise;} \end{cases}$$

(19)

The pheromone increase is represented by the equation above, and the bs indicator helps identify the best ant thus far. The rank-based variant of AS (referred to as AS Rank) is an addition to AS. Each ant in the AS rank makes a pheromone deposit, which diminishes with rank. Similar to the EAS approach, during each iteration, the ant that has found the best solution to the problem deposits the largest amount of pheromone.

### Control Strategy using Ant Colony Optimization tuned Fuzzy controller for Electric Vehicle

Fig. 6 Shows the Control Strategy of the Proposed Ant Colony optimized Fuzzy tuned PV, Battery & Super Capacitor fed Electric Vehicle. In this control the Reference voltage and DC bus voltage is compared and then the output signal from the comparator is processed through a PI controller. The signal from the PI controller & the State of charge of the super capacitor & the battery is fed as input to the Fuzzy logic controller through a gain block. Here the Ant colony optimization is used to tune the fuzzy logic controller and the output from the fuzzy block is processed through a gain and it is filtered. The ref current signal generated from the fuzzy is again compared with Battery & Super capacitor current values, it is output current signal is processed through Pi controller and the PWM pulses for the respective bidirectional converters are generated using the control technique.

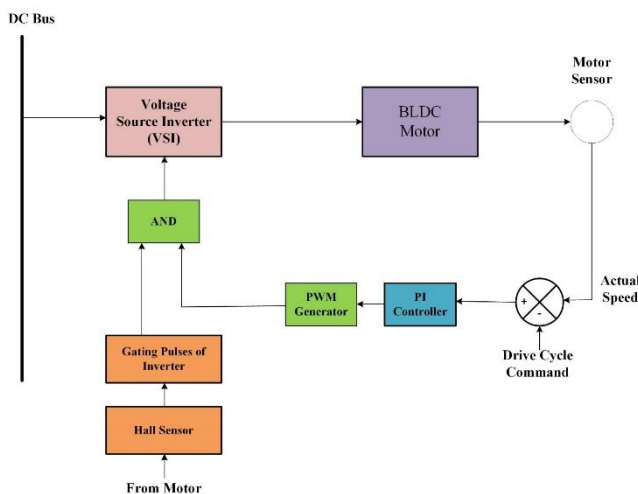


**Fig 7.** Closed loop Control of Electric Vehicle side BLDC motor

The Fig.7 shows the closed loop control of the Electric vehicle motor. Here the motor is connected to the DC bus through a inverter. The parameters of the motor is

monitored and the actual speed of the motor is compared with the drive cycle command it is processed through a PI controller and the output signal is generated, On the other hand a hall sensor is used to sense the gating pulsed of the inverter and the signal from the gating signal & PWM generated is given to the AND gate, thus the Controllers signal for the Voltage source inverter is generated.

### Simulation Results & Discussions

The simulation model of the ant colony optimization tuned fuzzy control for PV battery and super capacitor powered electric vehicle is crated and tested in the MATLAB Simulink software. The Simulink model of PV battery super capacitor based electric vehicle shown in Figure 8. The ant colony optimized fuzzy energy management and incremental conductance MPPT is shown in Figure 9.

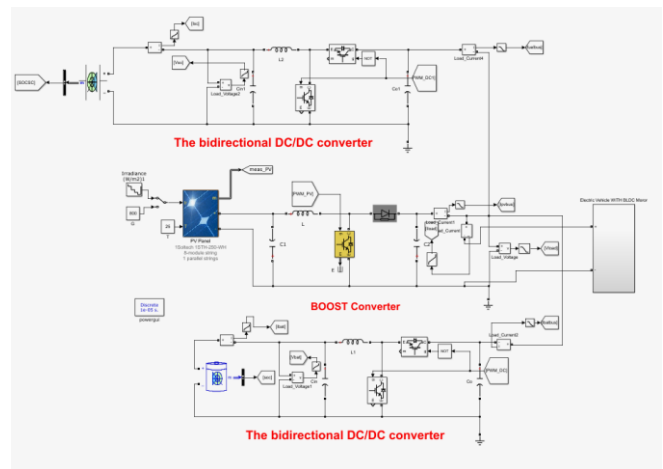


**Figure 8.** Simulink model PV battery and super capacitor powered electric vehicle

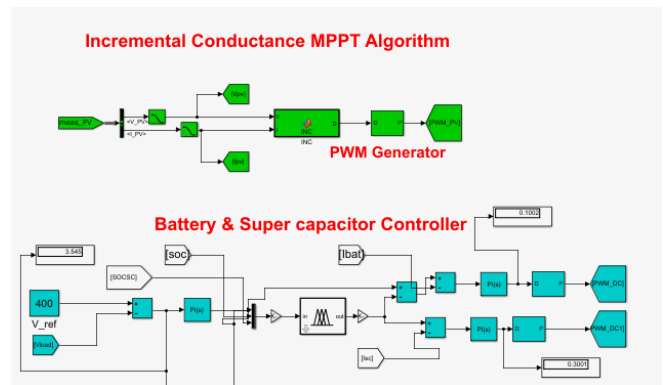


**Figure 9.** Simulink model proposed ant colony tuned fuzzy and incremental conductance MPPT system

The convergence graph of ant colony optimization for fuzzy tuning is shown in Figure 10. The ant colony optimization converges to global minimum at 5<sup>th</sup> iteration and tuned the fuzzy input and output scaling factor effectively. The scaling factor obtained by the ant colony optimization are 3.9493 and 3.4979.

The simulation of the proposed system tested with varying irradiance conditions such as irradiance change from 1



seconds from 1000, 800, 500, 300, 100 and corresponding results are measured and analyzed. Figure 11 shows the simulation results of the PV system such as voltage, current and power of the PV. The PV power is 2000 W at 1000 W/m<sup>2</sup> and it keep on decreasing with respect to decreasing irradiance. Figure 12 shows the simulation results of the battery system such as voltage, current and power of the battery. The battery voltage maintained at 350 volts and battery in charging mode from 0 to 1 seconds and discharging mode from 2 to 5 seconds due reduction in the PV power.

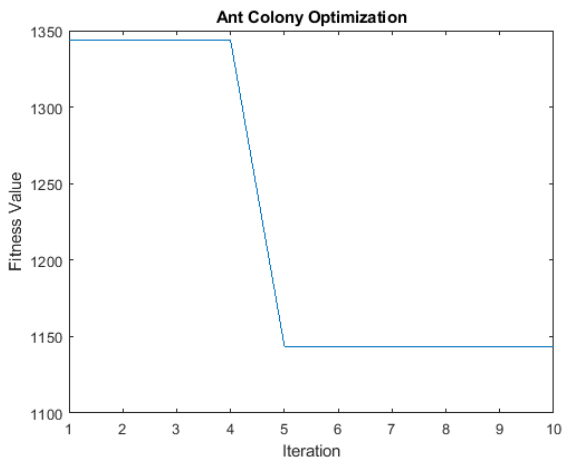


**Figure 10.** Convergence graph of Ant colony optimization

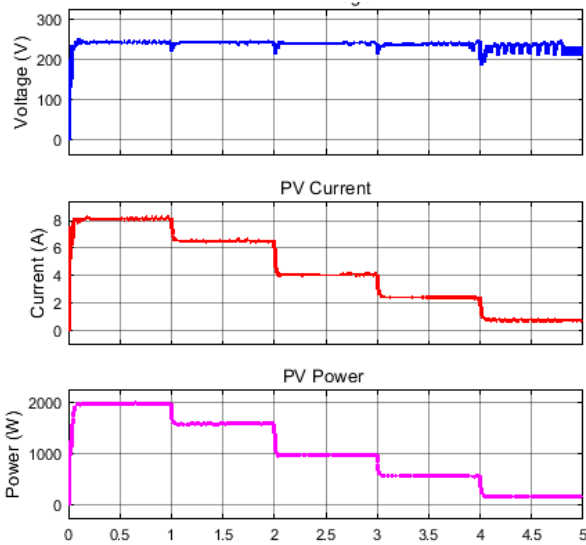


**Fig 11.** The simulation results of PV system

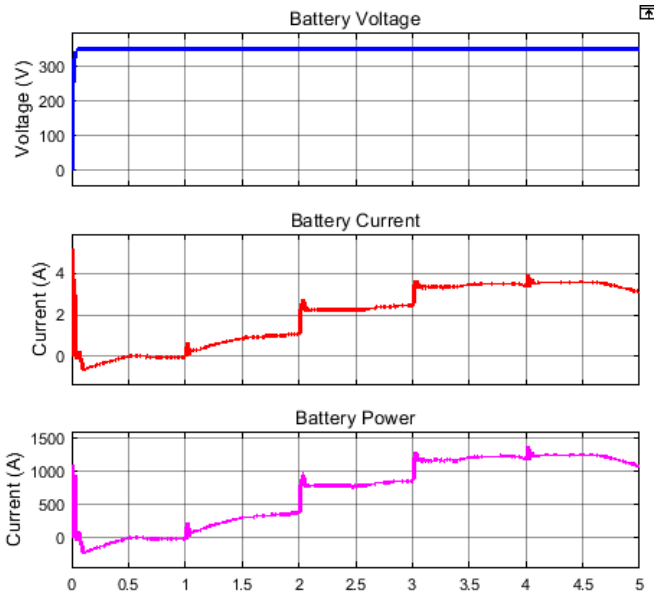


**Fig 12.** The simulation results of Battery system

Figure 13 shows the simulation results of the super capacitor system such as voltage, current and power of the battery. The battery voltage maintained at 250 volts and super capacitor in charging mode from 0 to 2 seconds and discharging mode during changing irradiance after 2 seconds.

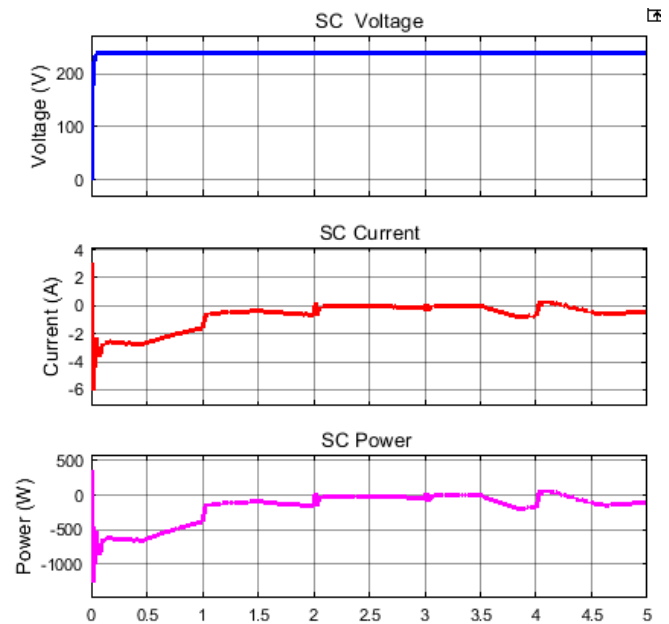


**Fig 13.** The simulation results of super capacitor system

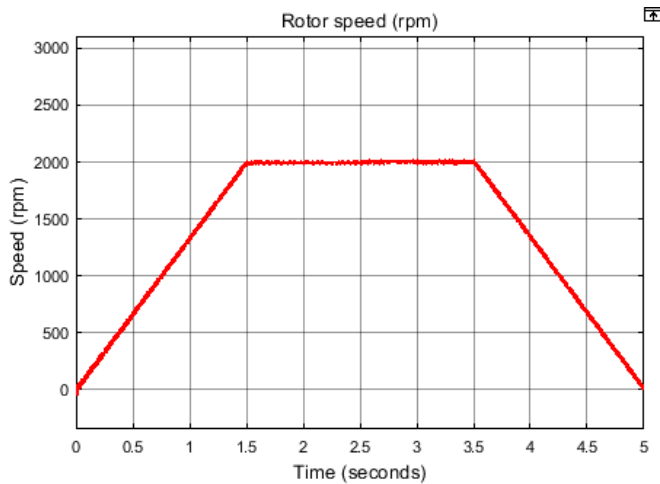


**Fig 14.** The simulation results of electric vehicle speed

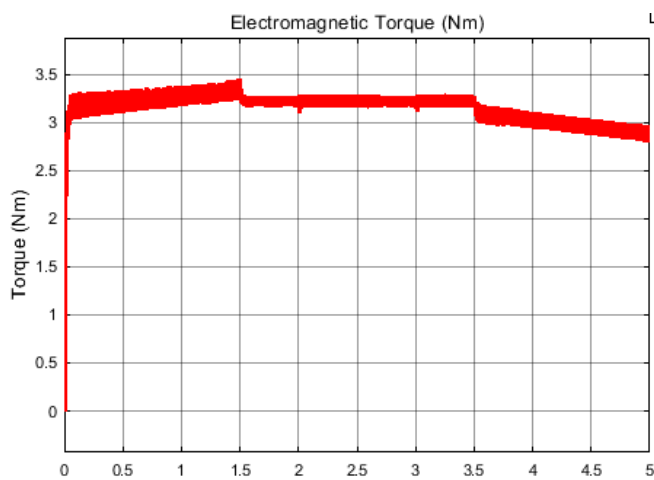


**Fig 15.** The simulation results of electric vehicle torque

Figure 14 and Figure 15 shows the simulation results of the electric vehicle speed and torque. The electric vehicle speed increase from 0 to 2000 rpm from 0 to 1.5 seconds and maintained at 2000 rpm from 1.5 to 3.5 seconds and then decrease to zero from 3.5 to 5 seconds. The torque of the electric vehicle maintained at 3.2 nm. The ant colony optimized fuzzy energy management effectively manage energy in the battery, electric vehicle and super capacitor with less power loss and high efficiency.

## Conclusion

This paper presents energy management in the PV super capacitor and battery based electric vehicle system using ant colony optimized fuzzy control system. The developed system was created and analyzed MATLAB Simulink software. The proposed system has been tested with different operating conditions such as changing irradiance conditions and change in electric vehicle speed conditions. the proposed energy management system effective control flow power among the super capacitor and battery and electric vehicle system with less power loss and high efficiency.

## References

- [1] Wang, Y., Lin, X., Kim, Y., *et al.*: ‘Architecture and control algorithms for combating partial shading in photovoltaic systems’, *IEEE Trans. Comput.- Aided Des. Integr. Circuits Syst.*, 2014, **6**, (33), pp. 917–930
- [2] Kanchev, H., Lu, D., Colas, F., *et al.*: ‘Energy management and operational planning of a microgrid with a PV-based active generator for smart grid applications’, *IEEE Trans. Ind. Electron.*, 2011, **10**, (58), pp. 4583–4592
- [3] Fakham, H., Lu, D., Francois, B.: ‘Power control design of a battery charger in a hybrid active PV generator for load following applications’, *IEEE Trans. Ind. Electron.*, 2011, **1**, (58), pp. 85–94
- [4] Wang, Y., Lin, X., Pedram, M.: ‘Adaptive control for energy storage systems in households with photovoltaic modules’, *IEEE Trans. Smart Grid*, 2014, **2**, (5), pp. 992–1001
- [5] Shin, D., Kim, Y., Wang, Y., *et al.*: ‘Constant-current regulator-based battery-supercapacitor hybrid architecture for high-rate pulsed load applications’, *J. Power Sources*, 2012, 205, pp. 516–52
- [6] Jiang, W., Zhang, L., Zhao, H., *et al.*: ‘Research on power sharing strategy of hybrid energy storage system in photovoltaic power station based on multi objective optimisation’, *IET Renew. Power Gener.*, 2016, 5, (10), pp. 575–583
- [7] Uzunoglu, M., Alam, M.S.: ‘Dynamic modeling, design, and simulation of a combined PEM fuel cell and ultracapacitor system for stand-alone residential applications’, *IEEE Trans. Energy Convers.*, 2006, **3**, (21), pp. 767–775
- [8] Roberts, B.P., Sandberg, C.: ‘The role of energy storage in development of smart grids’, *Proc. IEEE*, 2011, **6**, (99), pp. 1139–1144
- [9] Khaligh, A., Zhihao, L.: ‘Battery, ultracapacitor, fuel cell, and hybrid energy storage systems for electric, hybrid electric, fuel cell, and plugin hybrid electric vehicles: state-of-the-art’, *IEEE Trans. Veh. Technol.*, 2010, **6**, (59), pp. 2806–2814
- [10] Kyriakarakos, G., Dounis, A.I., Arvanitis, K.G., *et al.*: ‘A fuzzy logic energy management system for polygeneration microgrids’, *Renew. Energy*, 2012, **41**, pp. 315–327
- [11] M. Dorigo, T. Stutzle, *Ant Colony Optimization*, MIT Press, Cambridge, MA, 2004
- [12] D. Merkle, M. Middendorf, *Prospects for dynamic algorithm control: lessons from the phase structure of ant scheduling algorithms*, in: R.B. Heckendorn (Ed.),

Proceedings of the 2000 Genetic and Evolutionary Computation Conference – Workshop Program. Workshop “The Next Ten Years of Scheduling Research”, Morgan Kaufmann Publishers, Las Vegas, Nevada, USA, 2001

- [13] D. Merkle, M. Middendorf, H. Schmeck, Ant colony optimization for resource-constrained project scheduling, *IEEE Trans. Evol. Comput.* 6 (2002) 333–346.
- [14] B. Meyer, Convergence control in ACO, in: *Genetic and Evolutionary Computation Conference (GECCO)*, Seattle, WA, 2004.
- [15] J. Yen, R. Langari, *Fuzzy Logic: Intelligence, Control and Information*, Prentice Hall, 1999.